

## MULTIHEIGHT PROPERTIES OF MOVING MAGNETIC FEATURES

DEBI PRASAD CHOUDHARY<sup>1</sup> AND K. S. BALASUBRAMANIAM<sup>2</sup>

Received 2006 December 22; accepted 2007 April 12

### ABSTRACT

We report on spectropolarimetric and dynamical properties of a moving magnetic feature (MMF) around a disk-center sunspot observed using photospheric ( $\text{Fe I } \lambda\lambda 6301.5$  and  $6302.5$ ) and lower chromospheric ( $\text{Mg } b_2 \lambda 5172.7$ ) lines. We find that there are 33% fewer MMFs at the lower chromosphere compared to the photosphere, implying a sophisticated magnetic field geometry of tight low-level loops. A majority of bipolar MMFs are oriented with their neutral line perpendicular to the radial direction. Their “spot-ward” component has the same polarity as the sunspot. The magnetic filling factor is larger for all types of MMFs situated closer to the spot than those situated further away. Bipolar MMFs have a larger filling factor compared to the unipolar ones. Comparison of  $dI/d\lambda$  and Stokes  $V$  profile suggests a large magnetic filling factor within the MMFs in the photosphere. Traversing individual MMFs, the Stokes  $V$  profiles vary from normal antisymmetric structures to multilobed anomalous profiles. The chromospheric counterpart of multilobed and anomalous photospheric MMF Stokes  $V$  profiles are normal and antisymmetric. This suggests that magnetic loops corresponding to MMFs in the lower atmosphere are of mixed polarity and perhaps twisted while they are relatively relaxed in the corresponding upper atmosphere. The temporal evolution of the MMFs shows a transition between anomalous and normal Stokes  $V$  profiles.

*Subject headings:* Sun: chromosphere — Sun: magnetic fields — Sun: photosphere — sunspots

### 1. INTRODUCTION

Moving magnetic features (MMFs) occupy the interface between the coherent magnetic structure in sunspots and the surrounding turbulent photosphere (Harvey & Harvey 1973; Thomas et al. 2002; Hagenaar & Shine 2005). Observed mostly beyond the penumbral boundary, MMFs represent a cross section of highly inclined magnetic field lines that are immersed back into the photosphere. An early extensive study of the dynamical properties of these features was carried out at San Fernando Observatory by Dale Vrabec (1974), who showed that these features play different roles during the formation and decay phase of sunspots. High-resolution observations from ground and space show that many MMFs actually originate within the penumbra and enter the moat region following penumbral filaments (Cabrea Solana et al. 2006; Sainz Dalda & Martinez Pillet 2005; Ravindra 2006). Usually MMFs are observed as unipolar or bipolar *magnetic elements* beyond the penumbral region, moving away from the spot at a speed of about  $1\text{--}2 \text{ km s}^{-1}$  with a lifetime of a few hours. Models of sunspots point to MMFs as portions of the submerging flux tubes that interact with granular convection (Thomas et al. 2002; Zhang et al. 2003).

Sunspots appear to continually shed flux from the pore stage (Keil et al. 1999) to full-grown ones, as evidenced by innumerable *SOHO* MDI magnetogram movies. MMFs carry that flux, and are intricately related to the growth and evolution of sunspots. Hence, following their three-dimensional structure and dynamical behavior would help in formulating a mechanism for the formation and disappearance of sunspots. Further, there is observational evidence that several MMFs disappear due to flux cancellation as a consequence of magnetic reconnection in the photosphere (Bellot Rubio & Beck 2005). The reconnection related to MMFs could play a significant role in solar explosive events, as the emergence and disappearance of MMFs are also associated with flares and coronal mass ejections (Zhang & Wang 2002).

While morphological properties of MMFs have been studied using high-resolution observations, there is sparse information on their individual magnetic structure. Harvey & Harvey (1973), using low-resolution magnetograms, showed a lower limit for the magnetic flux in individual MMFs at about 300 G. Therein, they found similarities in MMFs observed in  $\text{Fe I } \lambda 5233$  and  $\text{Mg I } \lambda 5172.7$ , and a reasoned guess that the flux observed in  $\text{Mg I } \lambda 5172.7$  (formed higher in the atmosphere) was perhaps lower than that seen in  $\text{Fe I } \lambda 5233$ . No corresponding features of the MMFs were visible in the  $\text{H}\alpha$  line. More recently, Penn & Kuhn (1995) observed that MMFs do not rise to the height of  $\text{He I } \lambda 10830$  line formation (upper chromosphere). We report on magnetic field and spectropolarimetric properties of MMFs observed under high resolution, at two heights, using the Stokes profiles at the  $\text{Fe I } \lambda 6301.5$  and  $\text{Mg } b_2 \lambda 5172.7$  lines. There have been a number of studies related to the height of formation of these lines (Lites et al. 1988; Solanki & Bruls 1994; Mauas et al. 1988; Altrrock & Canfield 1974). The line-formation height is dependent on thermodynamic conditions which are complex in active regions. However, the solar atmosphere under varied model conditions shows that the contribution functions for  $\text{Fe I } \lambda 6301.5$  and  $\text{Mg } b_2 \lambda 5172.7$  lines are near the photosphere and chromosphere, respectively (Solanki & Bruls 1994; Lites et al. 1988). Here, we adopt the source of the observed two lines to be at photospheric and lower chromospheric heights of the solar atmosphere, separated by about 300 km.

### 2. OBSERVATIONS AND ANALYSIS

The observations of active region NOAA 9661 were carried out at the National Solar Observatory, in Sunspot, NM, with the Richard B. Dunn Solar Telescope (DST). Under excellent seeing conditions, we used the adaptive optics (AO) system and Advanced Stokes Polarimeter (ASP) during 2001 October 16–19. The details of the ASP instrument are well documented elsewhere (Elmore et al. 1992). We used an  $0.6''$  wide slit, which was  $1.6'$  long in the spatial direction orthogonal to the spectral dispersion. The slit was stepped with a sampling of  $0.36'' \text{ pixel}^{-1}$ . The ASP photospheric and chromospheric cameras were trained

<sup>1</sup> Mail Stop 8260, Department of Physics and Astronomy, California State University Northridge, Northridge, CA 91330; debiprasad.choudhary@csun.edu.

<sup>2</sup> National Solar Observatory, Sunspot, NM 88349; bala@nso.edu.

TABLE 1  
STATISTICAL PROPERTIES OF MMFs

Type	Photosphere	Chromosphere	Magnetic Field <sup>a</sup> (G)	Filling Factor $\alpha^a$
I.....	14	4	806	0.624
II.....	11	8	690	0.387
III.....	18	2	829	0.328

<sup>a</sup> Average values.

on the Fe I  $\lambda\lambda 6301.5$  and  $6302.5$  line pair and Mg  $b_2$   $\lambda 5172.7$  lines, respectively. The active region was scanned in 280 steps, which corresponds to a field of view of  $1.6' \times 2.8'$ . The spectral dispersions at 6300 and 5173 Å were 0.012 and 0.01 Å pixel<sup>-1</sup>.

The spectropolarimetric data were processed using the standard ASP routines (Skumanich et al. 1997). Here, we give a brief outline of the data analysis procedures adopted for the present paper. The instrumental artifacts were removed by subtracting dark frames and normalizing with “flat-field” images. The instrumental polarization introduced by the telescope and other reflecting optics was removed through a procedure using calibration images obtained during the observations. The calibrated data cube of spectra in polarized light that represents the Stokes  $I$ ,  $Q$ ,  $U$ , and  $V$  parameters were subjected to further data analysis for studying the properties of MMFs.

We used the ASP inversion code to derive various parameters of magnetic field from the Stokes profiles. The code uses a procedure of nonlinear least-squares fits of calibrated Stokes profiles obtained from the Unno-Rachkovsky solution for the polarized radiative transfer equation through Milne-Eddington atmosphere (Skumanich & Lites 1987). Among other quantities, the ASP inversion code gives the magnetic field strength ( $B$ ), magnetic field inclination with respect to the line of sight, and magnetic “fill factor”  $\alpha$ . Since the polarization profiles result from that fraction of observed element containing magnetic field, one can easily separate the fill factor by comparing these profiles with the total intensity, which is contributed by both magnetic and nonmagnetic fractions. Primarily the observed line profile,  $I_{\text{total}}(\lambda)$ , consists of two parts,  $I_{\text{nonmagnetic}}(\lambda)$  and  $I_{\text{magnetic}}(\lambda)$ , such that

$$I_{\text{total}}(\lambda) = (1 - \alpha)I_{\text{nonmagnetic}}(\lambda) + \alpha I_{\text{total}}(\lambda). \quad (1)$$

The procedure for the extraction of filling factor can be found in Lites & Skumanich (1990). In Table 1 we present the magnetic field strength and filling factor for different types of MMFs. It should be noted that the filling factor derived this way uses Unno-Rachkovsky solutions, which are purely symmetric, and asymmetric Stokes profiles. Such an assumption is blind to the information contained in the departure of line profile’s shape for symmetry and antisymmetry.

Alternately, the influence of filling factor can also be understood by examining the shape of line profiles. Using such a perspective, one can relate the derivative of intensity,  $dI/d\lambda$ , with the circular polarization profile,  $V$ , by weak field approximation:

$$V(\lambda) = CB\alpha \frac{dI}{d\lambda}, \quad (2)$$

where  $C$  is the spectral line constant. In such a comparison of actual line profiles, one would expect the Stokes  $V$  and  $dI/d\lambda$  profiles to closely resemble each other when the filling factors are high. With this approximation in mind, we examine three different kinds of profiles across MMF as shown in Figure 3. We will

discuss the implications of the differences between the Stokes  $V$  and  $dI/d\lambda$  profiles in the next section. One should note that examining the profiles this way helps us qualitatively understand the value of the filling factor derived from the ASP inversion. Since the chromospheric lines are not inverted because of the non-LTE complexity, one can understand the fill-factor influences on the chromospheric MMFs by comparing Stokes  $V$  and  $dI/d\lambda$ . Hence, we intend to apply this method to study the filling factor with chromospheric profiles where the inversion of Stokes profiles are more complex, which we discuss in the next section.

Active region NOAA 9661 had two well-developed sunspots of opposite polarity. It was located near solar disk center during observations on 2002 October 17. The eastern sunspot (S1) was circular, while the western (S2) was irregular (Fig. 1). We recorded five raster scans of the sunspot region in about 3 hr. The sunspot centers are marked by crosses. The umbra and penumbra boundaries were defined at 80% and 90% quiet Sun intensity in both wavelengths. The time-lapse animation of the five Fe I  $\lambda 6302.5$  Stokes  $V$  polarization images was used to identify the MMFs, which were moving radially away from the spots. We used MDI high-resolution magnetograms to cross verify that the identified features were indeed MMFs. The presence of chromospheric counterparts of MMFs were determined by examining the Mg  $b_2$  Stokes  $V$  profiles. We noted a positive identification when the Stokes  $V$  signal in the line core of the Mg  $b_2$  line was above  $2\sigma$  of the noise determined in the continuum window of the profile. Figure 1 shows images of the active region NOAA 9661 and the surrounding area in 6300.5 and 5172.6 Å, along with images in circular polarized light at 6301.7 and 5172.4 Å. The images in circular polarized light mimic the distribution of magnetic field polarity at photospheric and chromospheric heights in the field of view.

### 3. DISCUSSION

We discuss the dual-height statistical properties and filling-factor distribution of MMFs and their individual spatio-temporal properties.

#### 3.1. Statistical Properties and Compactness of MMFs

Several previous studies are consistent with a model in which the path of the magnetic flux tube originating from the sunspot forms an arch with a maximum height of about 300 km that enters the photosphere at a distance of 1500 km from the spot center (Degenhardt & Kneer 1992; Thomas et al. 2002). Using circular polarization images in the wings of Fe I  $\lambda 6302.5$  (photospheric) and Mg  $b_2$   $\lambda 5172.7$  (chromospheric) lines (Fig. 1), we estimate the height distribution of magnetic field arches. In general, we find that the photospheric polarization images (and line-of-sight magnetograms) show compact MMFs distributed throughout the field of view, while their chromospheric counterparts are diffuse. We categorize MMFs as type I (bipolar), II (unipolar of same polarity as the sunspot), and III (unipolar of opposite polarity with respect to the sunspot), similar to Thomas et al. (2002). The magnetic field of all three types of MMFs (Table 1), obtained from the ASP inversion code, ranges from about 100 to 1000 G, where the maximum field of the sunspot is about 4000 G. The average value of type II MMFs is lower compared to types I and III. All but one bipolar MMF (type I) are oriented such that their neutral line is perpendicular to the radial direction and the spotward component has the same polarity as the sunspot. This is consistent with the fact that MMFs are protruded penumbral flux tubes that are submerged as a result of granular convection. The number count of the MMFs at photospheric and chromospheric heights is given in Table 1. We find that fewer than 33% of MMFs are visible in the chromosphere, compared to their corresponding

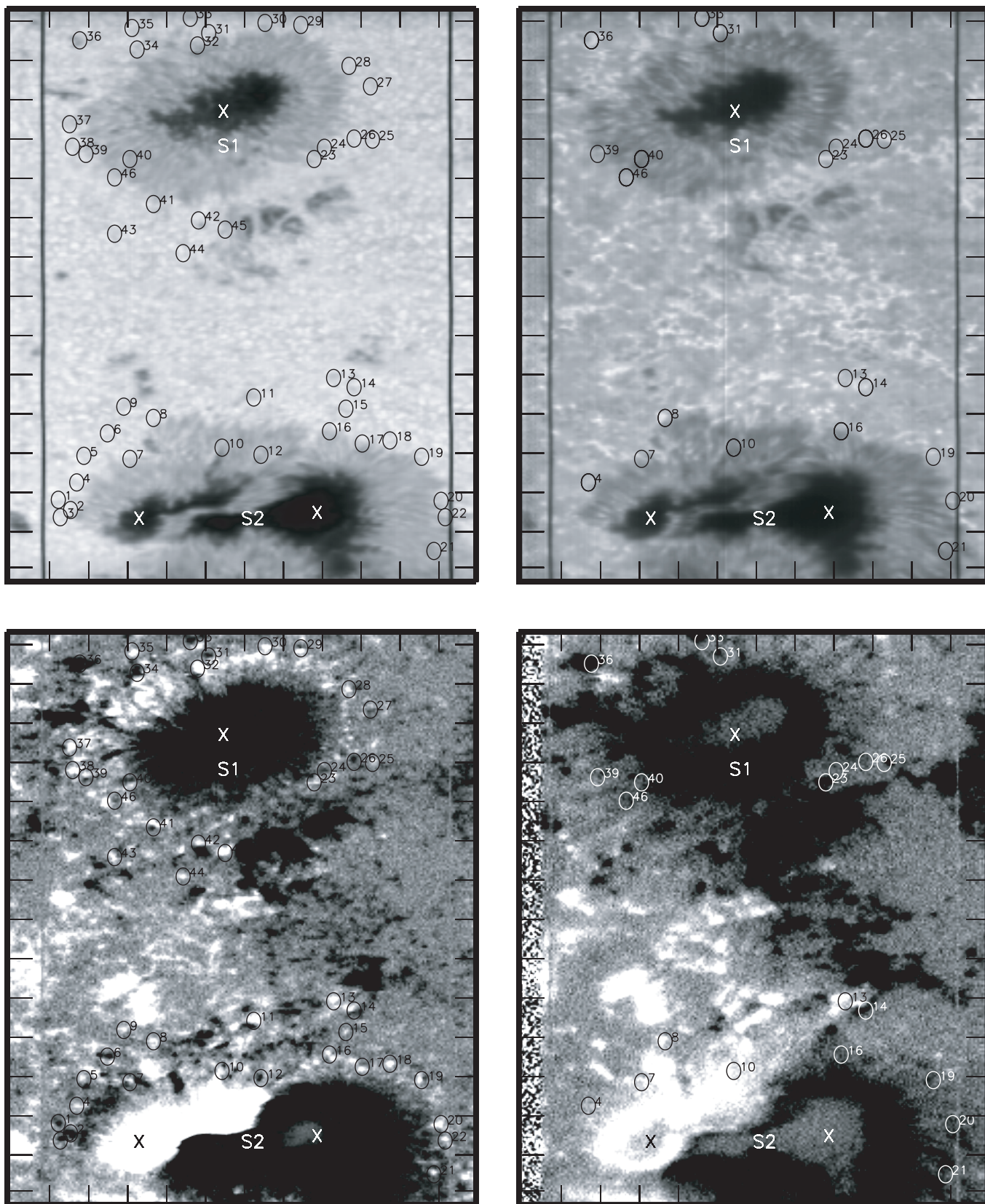


FIG. 1.—Images of the active region NOAA 9661 in the top panel are obtained at 6300.5 Å (*left*) and 5172.6 Å (*right*). The bottom panel shows circular polarization images at 6301.7 Å (*left*) and 5172.4 Å (*right*) and mimics the distribution of magnetic polarity in the field of view. The observations were taken on 2003 October 17 at 14:54 UT. The tick marks correspond to 10'' intervals.

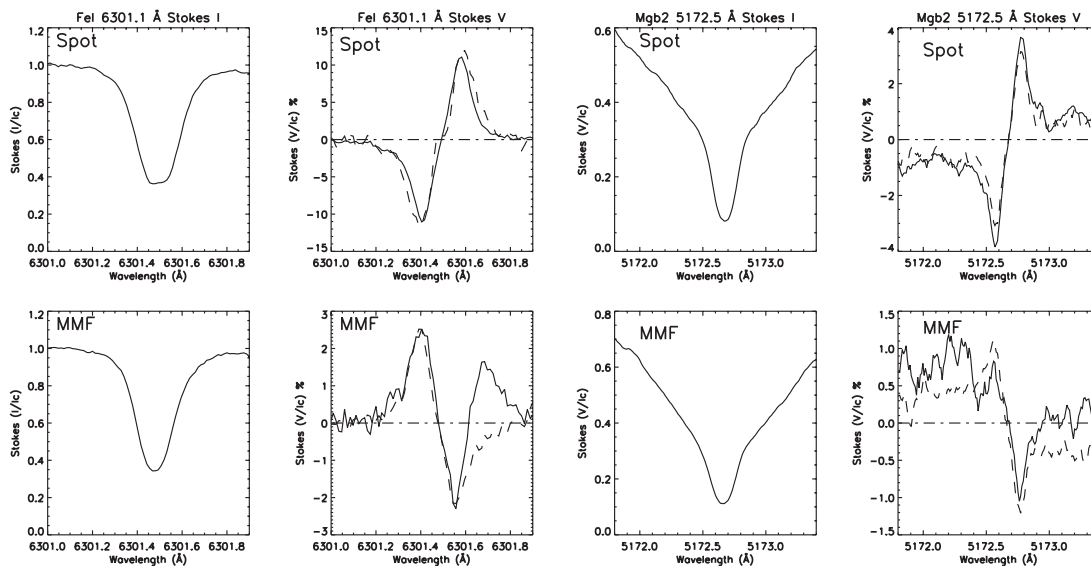


FIG. 2.—Stokes  $I$  and  $V$  profiles (solid lines) and  $dI/d\lambda$  (dashed lines) of active region NOAA 9661 obtained in photospheric Fe I and chromospheric Mg  $b_2$  lines. Top and bottom panels show the profiles in sunspot and MMFs. The Stokes  $V$  profiles are extracted from the same location in photosphere and chromosphere.

photospheric counterparts. A striking feature is that while the photospheric moat region contains compact MMFs of both polarities, such mixed-polarity MMFs are not observed in the chromospheric image. This implies that most of the MMFs do not reach the height of Mg  $b_2$  line formation. The only other possible explanation is that superpenumbral filaments in the chromosphere might obscure the tiny MMFs. However, from the intensity, magnetic, and velocity images of the Mg I  $\lambda 5172.7$  line, we do not see a significant superpenumbra (as seen in  $H\alpha$ ). This, coupled with a lack of identified MMFs either in 10830 Å or in  $H\alpha$ , as noted, favors a compact low-lying MMF magnetic structure. In case of type II, 8 out of 11 photospheric MMFs appear in the chromosphere. Among them, two photospheric MMFs (identified as numbers 26 and 24 in Fig. 1), which are situated at the edge of the continuum penumbra, are shifted radially outwards (from the sunspot center) by about  $1''$  in the chromosphere. Assuming the origin of the Mg  $b_2$  line at a height of about 300 km above the photosphere, this implies that the type II MMFs are highly inclined at an angle of about  $20^\circ$  to the photosphere.

### 3.2. MMF Stokes $V$ Profiles and their Spatio-Temporal Variation

Figure 2 shows Stokes  $I$ , the corresponding Stokes  $V$  (solid line), and  $dI/d\lambda$  (dashed line) line profiles of a sunspot umbra and an MMF. We observe three types of Stokes  $V$  profiles, one in which the area and amplitude of the blue and red lobes of the profile are same (balanced), a second category where the area and amplitudes of the blue and red lobes of the profile are different (unbalanced), and a third category where profiles have multiple lobes in one of the wings (anomalous). The noise ( $1\sigma$ ) of Stokes  $V$  profiles as determined in the continuum window in the sunspot and MMFs is about 0.015% for the photospheric lines and about 0.1% for the chromospheric lines. At most parts of the sunspot, the Stokes  $V$  profiles in both photosphere and chromosphere fit with the profile derived using equation (2). In the central part, where the magnetic field may not be in the weak field approximation range, the profiles do not match near the zero crossing. On the other hand, in the case of MMFs only the normal and asymmetric photospheric Stokes  $V$  profiles show such fitting. Their apparent similarities are due to suitable filling factors. We have independently determined the filling factor obtained from the full

and simultaneous inversion of Stokes profiles of Fe I 6301.5 and 6302.5 Å using the ASP inversion code. The average filling factors (averaged over an area around the circle shown in Fig. 1) are given in Table 1. Type I MMFs have a larger filling factor compared to types II and III. In general, MMFs closer to the spot center have a higher filling factor compared to the ones situated farther away. This may be due to the larger magnetic divergence of type II and III MMFs as a function of distance from the spot. Type I MMFs remain compact structures in the convective photosphere.

While we have not inverted full chromospheric spectral line profiles, we have examined the chromospheric Stokes profiles in the MMF and find that Stokes  $V$  profiles significantly depart from  $dI/d\lambda$ , indicating a lower filling factor. This may be due to the loosening of flux bundles as the MMF propagates upward and emerges in the chromosphere. However, we remind the reader that the filling factors discussed here are only photospheric filling factors determined using the full and simultaneous Stokes inversion of Fe I  $\lambda\lambda 6301.5$  and  $6302.5$  lines and also comparing the Stokes  $V$  profiles with  $dI/d\lambda$  profiles with an appropriate multiplicative constant. Both these approaches assume a homogeneous atmosphere that precludes the possible changes of magnetic field along the line of sight. In the case of anomalous Stokes  $V$  profiles, there is a gross mismatch between Stokes  $V$  and  $dI/d\lambda$  profiles. Such profiles are mostly observed in MMFs, indicating the presence of inhomogeneous magnetic fields.

The chromospheric MMF Stokes  $V$  profile at many locations shows the circular polarization signal over a broader wavelength interval compared to the sunspot profiles (Fig. 2). In particular, the chromospheric MMF Stokes  $V$  profiles show that the circular polarization signal is spread over the entire line profile of 1.5 Å, while the sunspot profiles show that the light is polarized within about 0.5 Å centered in the line core. Considering the  $1\sigma$  noise at 0.1% in the MMF Stokes  $V$  profiles shown in Figure 2, the departure is significant. We also note that the chromospheric Stokes  $I$  profiles are broader and asymmetric in the blue wing. These profiles indicate the nature of complex plasma dynamics at chromospheric heights. The significant contribution of the magnetic chromospheric profile (circular polarized light) in the blue wing could result in producing these observed Stokes  $V$  profiles. On the other hand, the photospheric MMF Stokes  $V$  profiles are mostly similar to the sunspot profiles unless they are anomalous.

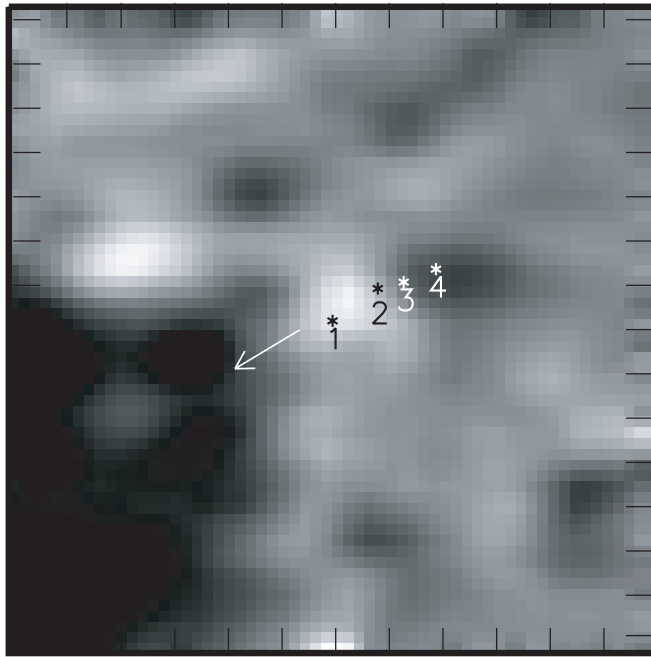


FIG. 3.— Spatial variation of Stokes  $V$  profiles (solid lines) within an MMF 28 shown in the center of the field of view of the image in the left. The dashed lines are  $dI/d\lambda$  profiles. Tick marks represent about  $2''$ . The profiles in the right are obtained from the positions in marked and numbered locations in the image. The arrow points toward the spot center.

As shown in Figure 2, the photospheric MMF Stokes  $V$  profiles at the polarity reversal line of the type-I MMFs always show an anomalous property. While the blue lobe of the profile is close to normal, the red lobe displays an anomalous property, perhaps indicating that the downward-moving magnetized plasma is discrete with complex dynamics.

Figures 3 and 4 demonstrate the spatial distribution of photospheric Stokes  $V$  profiles within an MMF and their temporal evolution at a fixed location, respectively. As previously mentioned, the photospheric Stokes  $V$  profiles at the polarity reversal

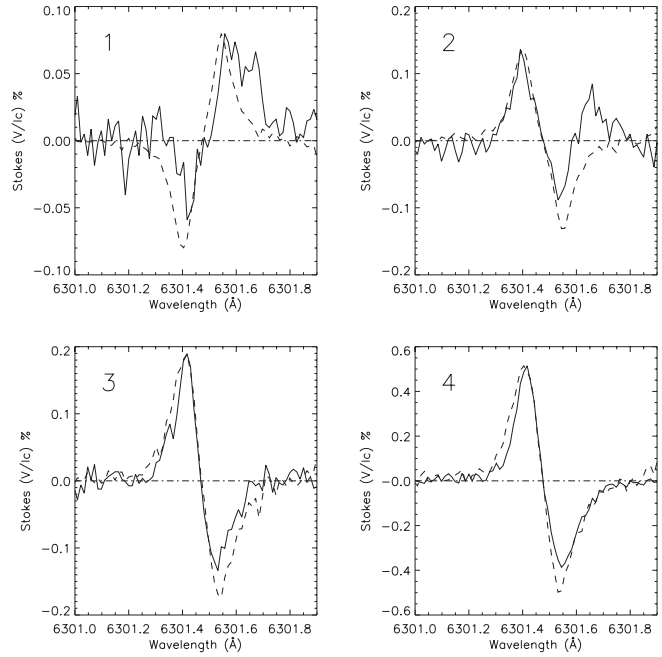


FIG. 4.— Stokes  $V$  profiles (solid lines) at location 1 of MMF 28 of the active region NOAA 9661 observed in successive data sets on 2001 October 17. The dashed lines are  $dI/d\lambda$  profiles. The time on each profile corresponds to the beginning of the ASP scan for each observation.

line of type I MMFs show anomalous profiles. Occasionally, other MMFs also show such profiles. In all five scans spatially traversing these types of MMFs, the profiles frequently change to excessive red-lobed anomalous profiles. It is tempting to interpret this change as the temporal variability of the type I MMF neutral lines. However, we recognize that the temporal cadence of about 30 minutes is too long to allow a definite conclusion. Assuming that the temporal changes in the sequence of Stokes  $V$  profiles might be due to the dynamical nature of magnetized plasma, the possibility of spatial and temporal mixing to create multilobed profiles was examined in the MMFs from the subsequent frames. We do not see any of the Stokes  $V$  profiles that correspond to the profiles of previous frames. If the spatial displacement of an MMF were responsible instead of temporal plasma dynamics, we would expect the previous profile to be present nearby, which is contrary to the observations. Although this indicates the predominantly temporal character of changing profiles on successive frames, the motion of MMFs could still cause confusion with temporal changes. In this case, as the MMFs move each element may not fall into spatially resolvable pixels, thereby contributing to spatial mixing. In any case, one can infer that the temporal changes of Stokes  $V$  profiles indicate both time variation and spatial complexity of magnetized plasma in MMFs. It is important to note that such anomalous Stokes  $V$  profiles are not observed at chromospheric heights.

Asymmetric and anomalous Stokes profiles have been previously observed by several authors in the quiet Sun (Sigwarth et al. 1999), and in penumbrae and light bridges (Sanchez Almeida & Lites 1992; Balasubramaniam et al. 1997; Sankarasubramanian & Rimmele 2002; Degenhardt & Kneer 1992; Schlichenmaier & Collados 2002). The inversion codes that assume constant magnetic and velocity fields can reproduce symmetric and antisymmetric Stokes  $V$  profiles. However, in order to reproduce the anomalous profiles it is necessary to consider the inhomogeneities of magnetic field, velocity, and temperature in the solar atmosphere. Inclusion of such properties is made by sophisticated inversion codes that take into account the variation of magnetic field with depth, e.g., microstructured magnetic atmosphere (MISMA) by Sanchez

Almeida (1997, 2000, 2005) and Stokes Inversion based on Response functions (SIR) by Ruiz Cobo & del Toro Iniesta (1992). Anomalous profiles in the quiet Sun are also observed in Fe I  $\lambda\lambda 6301.5$  and  $6302.5$  and Fe I  $\lambda 15652.874$  and explained using the MISMA hypothesis (Dominguez Cerdena et al. 2006). The observed anomalous profiles across the neutral line of bipolar MMFs could be due to the following reason. As described by Thomas et al. (2002), MMFs are the cross section of penumbral flux that is protruded through the photosphere, and interact with the surrounding photosphere. This interaction between the penumbral magnetic flux and granular convection in the surrounding photosphere produce temporally varying complex magnetic structures. The penumbral flux carries moving plasma that is observed in Evershed flow. The interaction between the moving plasma in the penumbral flux bundle and granular convection could produce complex magnetic loops that might manifest in the form of unresolved mixed polarities along the line of sight and produce the observed anomalous Stokes  $V$  profiles. In a model of sunspot and penumbral structure by Schlichenmaier (2002), the time-dependent properties of the interaction of the penumbral flux tube with the photosphere is analogous to a “photospheric serpent.” Such a model predicts the up and down flow of plasma with different temperatures for the crests and troughs. The anomalous Stokes  $V$  profiles could also be produced by the magnetized plasma of different temperatures, at crests and troughs of the flux tube. A detailed analysis and an inversion of profiles to reproduce multi-component temperature, velocity, and magnetic fields might help to understand such structures. We plan to make such an analysis in the future.

#### 4. SUMMARY

These ASP observations of active region NOAA 9661 in photospheric Fe I  $\lambda\lambda 6301.5$  and  $6302.5$  and chromospheric Mg  $b_2$

$\lambda 5172.7$  lines show that most bipolar MMFs have their neutral line perpendicular to the radial direction and the spot-ward component has the same polarity as the sunspot. There are 33% fewer MMFs in the chromosphere compared to the photosphere, implying that most of the MMFs do not reach the lower chromosphere. The MMF filling-factor study shows that the flux is loosely bound as it propagates toward the upper atmosphere. There is a varied flux density in different types of MMFs at different distances from the sunspot. The MMF photospheric Stokes  $V$  profiles have an anomalous red component unlike their chromospheric counterpart, which could be due to a complex spatial and thermodynamical properties of down-flowing magnetized plasmas. Similarly, we also observe the temporal evolution of the MMFs showing the transition between anomalous and normal Stokes  $V$  profiles. Our observations show the complexity of MMFs within the resolvable spatial and temporal scale, the entanglement of which could often lead to the destabilization of magnetic structures in the solar atmosphere. With consistent higher spatial and sustained temporal observations with the *Hinode* mission, we plan to further investigate the nature of these objects.

This work was partially supported by NSF grant ATM-0548260 and Cottrell College Science Award CC6496. The National Solar Observatory is operated by the Association of Universities for Research in Astronomy for the NSF. We thank Doug Gilliam, Joe Elrod, and Mike Bradford for valuable observing support. We acknowledge the use of the HAO/NSO Advanced Stokes Polarimeter. We thank Gary Chapman, Angie Cookson, and Dora Preminger of San Fernando Observatory, Department of Physics and Astronomy at CSUN for helping to improve the presentation. We thank the referee for useful comments.

#### REFERENCES

- Altrock, R. C., & Canfield, R. C. 1974, *ApJ*, 194, 733  
 Balasubramanian, K. S., Keil, S. L., & Tomczyk, S. 1997, *ApJ*, 482, 1065  
 Bellot Rubio, L., & Beck, C. 2005, *ApJ*, 626, L125  
 Cabrera Solana, D., Bellot Rubio, L., Beck, C., & del Toro Iniesta, J. C. 2006, *ApJ*, 649, L41  
 Degenhardt, D., & Kneer, F. 1992, *A&A*, 260, 411  
 Dominguez Cerdena, I., & Sanchez Almeida, J. 2006, *ApJ*, 646, 1421  
 Elmore, D. F., et al. 1992, *Proc. SPIE* 1746, 22  
 Hagenaar, H. J., & Shine, R. A. 2005, *ApJ*, 635, 659  
 Harvey, K., & Harvey, J. 1973, *Sol. Phys.*, 28, 61  
 Keil, S. L., Balasubramanian, K. S., Smaldone, L. A., & Reger, B. 1999, *ApJ*, 510, 422  
 Lites, B. W., & Skumanich, A. 1990, *ApJ*, 348, 747  
 Lites, B. W., Skumanich, A., Rees, D. E., & Murphy, G. A. 1988, *ApJ*, 330, 493  
 Mauas, J., Avrett, H., & Loeser, R. 1988, *ApJ*, 330, 1008  
 Penn, M. J., & Kuhn, J. R. 1995, *ApJ*, 441, L51  
 Ravindra, B. 2006, *Sol. Phys.*, 237, 297  
 Ruiz Cobo, B., & del Toro Iniesta, J. C. 1992, *ApJ*, 398, 375  
 Sainz Dalda, A., & Martinez Pillet, V. 2005, *ApJ*, 632, 1176  
 Sanchez Almeda, J. 1997, *ApJ*, 491, 993  
 ———. 2000, *ApJ*, 532, 1215  
 ———. 2005, *ApJ*, 622, 1292  
 Sanchez Almeda, J., & Lites, B. W. 1992, *ApJ*, 398, 359  
 Sankarasubramanian, K., & Rimmele, T. 2002, *ApJ*, 576, 1048  
 Schlichenmaier, R. 2002, *Astron. Nachr.*, 323, 303  
 Schlichenmaier, R., & Collados, M. 2002, *A&A*, 381, 668  
 Sigwarth, M., Balasubramanian, K. S., Knolker, M., & Schmidt, W. 1999, *A&A*, 349, 941  
 Skumanich, A., Lites, B. W., Martinez Pillet, V., & Seagraves, P. 1997, *ApJS*, 110, 357  
 Solanki, S. K., & Bruls, J. H. M. J. 1994, *A&A*, 286, 269  
 Thomas, J. H., Weiss, N. O., Tobias, S. M., & Brummell, N. H. 2002, *Nature*, 420, 390  
 Vrabc, D. 1974, in *Proc. IAU Symp. 56, Chromospheric Fine Structure*, ed. R. G. Athay (Dordrecht: Reidel), 201  
 Zhang, J., Solanki, S. K., & Wang, J. 2003, *A&A*, 399, 755  
 Zhang, J., & Wang, J. 2002, *ApJ*, 566, L117